

One-Pot and Step-by-Step N-Assisted C_{Ph}–H Activation in 2-(4-Bromophenyl)imidazol[1,2-*a*]pyridine: Synthesis of a New C,N-Cyclometalated Compound [$\{\text{Pt}(\text{C}^{\wedge}\text{N})(\mu\text{-Cl})\}_2$] as Precursor of Luminescent Platinum(II) Compounds

Juan Forniés,^{*,†} Violeta Sicilia,^{*,‡} Carmen Larraz,[†] José A. Camerano,[†] Antonio Martín,[†] José M. Casas,[†] and Athanassios C. Tsipis^{*,§,⊥}

[†]*Departamento de Química Inorgánica, Instituto de Ciencia de Materiales de Aragón, Facultad de Ciencias, Universidad de Zaragoza–CSIC, Plaza. S. Francisco s/n, 50009, Zaragoza, Spain,* [‡]*Departamento de Química Inorgánica, Instituto de Ciencia de Materiales de Aragón, Escuela Universitaria de Ingeniería Técnica Industrial, Universidad de Zaragoza–CSIC, Campus Universitario Río Ebro, Edificio Torres Quevedo, 50018, Zaragoza, Spain,* and [§]*Laboratory of Inorganic and General Chemistry, Department of Chemistry, University of Ioannina, 451 10 Ioannina, Greece*

Received November 30, 2009

The activation of a C_{Ph}–H bond in the phenyl ring of 2-(4-bromophenyl)imidazol[1,2-*a*]pyridine (HC[^]N) by [$\{\text{Pt}(\eta^3\text{-C}_4\text{H}_7)(\mu\text{-Cl})\}_2$] ($\eta^3\text{-C}_4\text{H}_7 = \eta^3\text{-2-methylallyl}$) renders the new cyclometalated complex [$\{\text{Pt}(\text{C}^{\wedge}\text{N})(\mu\text{-Cl})\}_2$] (**2**) with high yield and selectivity. Complex **2** can be achieved directly in a one-pot reaction or step by step through the intermediate [$\text{Pt}(\eta^3\text{-C}_4\text{H}_7)\text{Cl}(\text{HC}^{\wedge}\text{N-}\kappa\text{N})$] (**1**). Compound **1** could be isolated and fully characterized. The X-ray structure shows the coordination of HC[^]N through only the N and the existence of a weak Pt···H–C hydrogen bridging bond (Pt···H1 = 2.78 Å, Pt···C1 = 3.365(3) Å, Pt–H1–C1 = 120.9°). Hence, the formation of this intermediate could be considered the first step in the cyclometalation process. The mononuclear complexes [$\text{PtCl}(\text{C}^{\wedge}\text{N})\text{L}$] (L = tht (**3**), PPh₃ (**4**), CN-Xyl (**5**), CN-^tBu (**6**)) were obtained by cleavage of the bridging system in [$\{\text{Pt}(\text{C}^{\wedge}\text{N})(\mu\text{-Cl})\}_2$] (**2**) by the neutral ligands, L. The resulting geometry (*trans* C, Cl) is that expected from the electronic preferences, taking into account the degree of transphobia (*T*) of pairs of *trans* ligands, $T[\text{C}(\text{C}^{\wedge}\text{N})/\text{L}(\text{Cl})] < T[\text{C}(\text{C}^{\wedge}\text{N})/\text{L}(\text{S}, \text{P}, \text{C})]$. Complexes [$\text{PtCl}(\text{C}^{\wedge}\text{N})\text{L}$] (L = CN-Xyl (**5**), CN-^tBu (**6**)) containing two strong-field ligands, a C_CN σ-bonded and an isocyanide ligand, are luminescent. TD-DFT calculations were performed for the singlet ground state, S₀, as well as for the first triplet excited state of **6** in both the gas phase and solution. Calculations indicate that the lowest-lying absorption involves mainly ¹IL (C[^]N) mixed with a small contribution of ¹MLCT/¹L/LCT (L = C[^]N; L' = Cl) transitions. Complex **5** exhibits “*luminescent thermochromism*” in the solid state; at 77 K it shows a green phosphorescence band assigned to ³IL transitions located on the C[^]N group of monomer species, while at 298 K an orange-red emission is observed, being tentatively assigned to excited states of emissive aggregates (³MMLCT/³π–π*). However complex **6** shows phosphorescence only at 77 K both in solution and in the solid state with the emissions arising from ³IL and ³L'MLCT excited states of monomer species.

Introduction

Transition metal cyclometalated compounds containing five-membered metallacycles can be selectively synthesized as compared to other sized ring compounds. They are very stable organometallic compounds due to the chelating effect and have been known for a long time.^{1–3} The great interest in

this kind of compound has been mainly due to their application as reagents for highly regioselective organic synthesis or as catalysts for cross-coupling, alkane dehydrogenation, or Diels–Alder reactions, among others.^{1,4,5} More recently, the increasing attention paid to transition metal cyclometalated compounds is due to their attractive photochemical and photophysical properties^{6–8} and their potential use as molecular devices.

*Corresponding authors. E-mail: juan.fornies@unizar.es. Fax: (+34)976-761187.

[⊥]Corresponding author regarding the TD-DFT calculations. E-mail: attsipis@cc.uoi.gr.

(1) Omae, I. *Coord. Chem. Rev.* **2004**, *248*, 995.
(2) Mohr, F.; Privér, S. H.; Bhargava, S. K.; Bennett, M. A. *Coord. Chem. Rev.* **2006**, *250*, 1851.
(3) Crabtree, R. H.; Mingos, D. M. P. *Comprehensive Organometallic Chemistry III*; Crabtree, R. H., Mingos, D. M. P., Eds.; Elsevier: Oxford, 2007.

(4) Zhu, K.; Achord, P. D.; Zhang, X.; Krogh-Jerpersen, K.; Goldman, A. S. *J. Am. Chem. Soc.* **2004**, *126*, 13044.
(5) Omae, I. *J. Organomet. Chem.* **2007**, *692*, 2608.
(6) Lowry, M. S.; Bernhard, S. *Chem.–Eur. J.* **2006**, *12*, 7970.
(7) Termine, R.; Talarico, M.; Aiello, I.; Dattilo, D.; Pucci, D.; Ghedini, M.; Golemme, A. *Opto-Electron. Rev.* **2005**, *13*, 287.
(8) Santoro, A.; Whitwood, A. C.; Williams, J. A. G.; Kozhevnikov, V. N.; Bruce, D. W. *Chem. Mater.* **2009**, *21*, 3871.

In the transition metal complexes of C,N-cyclometalated ligands the presence of π -conjugated fragments around the metal ion gives rise to ligand-centered (IL, π - π^* , or n - π^*) and metal-to-ligand charge transfer (MLCT) excited states, the lowest unoccupied molecular orbital (LUMO, π^*) being located mainly on the imine fragment, which lies at lower energies than the d-d states. Moreover, the strong σ -donor C_CN atom affords the metal ion a very strong ligand field, raising the energy of the nonradiative metal-centered (d-d) excited states to relatively inaccessible energies. Additionally, the introduction of strong-field ancillary ligands in the complex increases the energy gap, ΔE , between the lowest-lying excited state (IL/ MLCT) and higher-lying d-d state, so the nonradiative decay is inhibited. Thus, many isolated C,N-cyclometalated Pt(II) complexes emit from ³IL and/or ³MLCT states and are luminescent in solution under ambient conditions.^{9–12} Some of them have been successfully applied in the manufacture of photosensors or phosphorescent organic light-emitting devices (PhOLEDs).^{9,11–21}

Mononuclear heteroleptic complexes with a single cyclometalating ligand (C[^]N) allow the fine-tuning of photophysical properties via variation of the electronic nature (donating or withdrawing character) of the cyclometalating or even the ancillary ligands.²² The electronic properties of the ligands affect the electron density at the metal center and consequently force the metal-to-ligand charge transfer (MLCT) transitions to be mixed with the lowest-energy transitions, thus altering the relative energy, radiative color, and lifetime of the excited state.^{23–25} This is the case, for example, in heteroleptic benzoquinolate Pt(II) complexes

with phosphine,²⁶ alkylphosphine,²⁶ alkynyl,²⁷ cyanide,²⁸ and isocyanide²⁹ as ancillary ligands. In addition, Pt(II) complexes with sterically undemanding ligands are essentially flat, and therefore ground- and excited-state interactions become feasible depending on the concentration and proximity of the molecules. This fact leads to marked red-shifted phosphorescence transitions with respect to those in the monomer species. These transitions are assigned to metal–metal-to-ligand charge transfer (MMLCT) or excimeric ligand-to-ligand charge transfer and are highly dependent on the extent of Pt···Pt and π ··· π interactions.^{9,10,30–32}

Following on with our interest in the chemistry and photophysical properties of cyclometalated Pt(II) compounds,^{28,29,33,34} our aim was to prepare new luminescent compounds via variation of the cyclometalating ligand. Along these lines, we describe the cyclometalation of 2-(4-bromophenyl)imidazol[1,2-*a*]pyridine (HC[^]N) by $[\{\text{Pt}(\eta^3\text{-C}_4\text{H}_7)(\mu\text{-Cl})\}_2]$ ($\eta^3\text{-C}_4\text{H}_7 = \eta^3\text{-2-methylallyl}$) as a one-pot or step-by-step reaction, through the intermediate $[\text{Pt}(\eta^3\text{-C}_4\text{H}_7)\text{Cl}(\text{HC}^{\wedge}\text{N}-\kappa\text{N})]$, to yield the di- μ -chloro cyclometalated compound $[\{\text{Pt}(\text{C}^{\wedge}\text{N})(\mu\text{-Cl})\}_2]$. This dinuclear compound was used as starting material for the synthesis of the mononuclear complexes $[\text{PtCl}(\text{C}^{\wedge}\text{N})\text{L}]$ (L = tht, PPh₃, CNXyl, CNBut), which incorporate monodentate ligands with different electron-withdrawing/donating properties, in order to tune the emission properties. As expected, only complexes **5** and **6**, containing the strong-field isocyanide ligand, are luminescent. Their photophysical properties were thoroughly investigated. To gain a better understanding of the nature of the absorption and emission bands, time-dependent density functional theory (TD-DFT) calculations were performed for the singlet ground state, S₀, as well as for the first triplet excited state of **6** in both the gas phase and solution.

Results and Discussion

Reaction of $[\{\text{Pt}(\eta^3\text{-C}_4\text{H}_7)(\mu\text{-Cl})\}_2]$ with 2-(4-Bromophenyl)imidazol[1,2-*a*]pyridine (HC[^]N). Synthesis of $[\text{Pt}(\eta^3\text{-C}_4\text{H}_7)\text{Cl}(\text{HC}^{\wedge}\text{N})]$ (1**) and $[\{\text{Pt}(\text{C}^{\wedge}\text{N})(\mu\text{-Cl})\}_2]$ (**2**) Compounds.** When a solution of the dichloro-bridged complex $[\{\text{Pt}(\eta^3\text{-C}_4\text{H}_7)(\mu\text{-Cl})\}_2]$ ($\eta^3\text{-C}_4\text{H}_7 = \eta^3\text{-2-methylallyl}$) and an equimolar amount of 2-(4-bromophenyl)imidazol[1,2-*a*]pyridine (HC[^]N) was refluxed in acetone (Scheme 1a and Experimental Section for details), compound $[\text{Pt}(\eta^3\text{-C}_4\text{H}_7)\text{Cl}(\text{HC}^{\wedge}\text{N})]$ (**1**) precipitated as a white solid. However, by refluxing a solution containing equimolar amounts of the allyl complex $[\{\text{Pt}(\eta^3\text{-C}_4\text{H}_7)(\mu\text{-Cl})\}_2]$ and HC[^]N in 2-methoxyethanol (Scheme 1b and Experimental Section for details), the precipitated solid corresponded to complex $[\{\text{Pt}(\text{C}^{\wedge}\text{N})(\mu\text{-Cl})\}_2]$ (**2**). Complex **2** can be also obtained by refluxing a suspension of compound **1** in 2-methoxyethanol (Scheme 1c). Compound **1** was isolated as a pure, air-stable solid and fully characterized (see Experimental Section). A $\nu_{\text{Pt-Cl}}$ absorption (285 cm⁻¹) is consistent with the presence

(9) Williams, J. A. G.; Develay, S.; Rochester, D. L.; Murphy, L. *Coord. Chem. Rev.* **2008**, *252*, 2596.

(10) Williams, J. A. G. *Top. Curr. Chem.* **2007**, *281*, 205.

(11) Grosby, G. A.; Kendrick, K. R. *Coord. Chem. Rev.* **1998**, *17*, 407.

(12) Chou, P. T.; Chi, Y. *Chem.—Eur. J.* **2007**, *13*, 380.

(13) Xiang, H. F.; Lai, S. W.; Lai, P. T.; Che, C. M. Phosphorescent platinum(II) materials for OLED applications. In *Highly Efficient OLEDs with Phosphorescent Materials*; Yersin, H., Ed.; Wiley-VCH: Weinheim, 2007.

(14) Evans, R. C.; Douglas, P.; Winscom, C. J. *Coord. Chem. Rev.* **2006**, *250*, 2093.

(15) Thomas, S. W.; Venkatesan, K.; Mullar, P.; Swager, T. M. J. *Am. Chem. Soc.* **2006**, *128*, 16641.

(16) Lai, S. W.; Che, C. M. *Top. Curr. Chem.* **2004**, *241*, 27.

(17) He, Z.; Wong, W. Y.; Yu, X.; Kwok, H. S.; Lin, Z. *Inorg. Chem.* **2006**, *45*, 10922.

(18) Koo, C.-K.; Ho, Y.-M.; Chow, C.-F.; Lam, M. H.-W.; Lau, T.-C.; Wong, W.-Y. *Inorg. Chem.* **2007**, *46*, 3603.

(19) Williams, J. A. G.; Wilkinson, A. J.; Whittle, V. L. *Dalton Trans.* **2008**, 2081.

(20) Williams, J. A. G. *Chem. Soc. Rev.* **2009**, *38*, 1783.

(21) Lau, K. S. F.; Zhao, S.; Ryppa, C.; Jockusch, S.; Turro, N. J.; Zeller, M.; Gouterman, M.; Khalil, G. E.; Brückner, C. *Inorg. Chem.* **2009**, *48*, 4067.

(22) Hwang, F.-M.; Chen, H.-Y.; Chen, P.-S.; Liu, C.-S.; Chi, Y.; Shu, C.-F.; Wu, F.-I.; Chou, P. T.; Peng, S.-M.; Lee, G.-H. *Inorg. Chem.* **2005**, *44*, 1344.

(23) You, Y.; Seo, J.; Kim, S. H.; Kim, K. S.; Ahn, T. K.; Kim, D.; Park, S. Y. *Inorg. Chem.* **2008**, *47*, 1476.

(24) Zhang, K.; Hu, J.; Chan, K. C.; Wong, K. Y.; Yip, J. H. K. *Eur. J. Inorg. Chem.* **2007**, 384.

(25) You, Y.; Kim, K. S.; Ahn, T. K.; Kim, D.; Park, S. Y. *J. Phys. Chem. C* **2007**, *111*, 4052.

(26) Díez, A.; Forniés, J.; García, A.; Lalinde, E.; Moreno, M. T. *Inorg. Chem.* **2005**, *44*, 2443.

(27) Fernández, S.; Forniés, J.; Gil, B.; Gómez, J.; Lalinde, E. *Dalton Trans.* **2003**, 822.

(28) Forniés, J.; Fuertes, S.; López, J. A.; Martín, A.; Sicilia, V. *Inorg. Chem.* **2008**, *47*, 7166.

(29) Díez, A.; Forniés, J.; Fuertes, S.; Lalinde, E.; Larraz, C.; López, J. A.; Martín, A.; Moreno, M. T.; Sicilia, V. *Organometallics* **2009**, *28*, 1705.

(30) Yam, V. W. W.; Wong, K. M. C.; Zhu, N. J. *Am. Chem. Soc.* **2002**, *124*, 6506.

(31) Yam, V. W. W.; Chan, K. H. Y.; Wong, K. M. C.; Chu, B. W. K. *Angew. Chem., Int. Ed.* **2006**, *45*, 6169.

(32) Moussa, J.; Wong, K. M. C.; Chamoreau, L. M.; Amouri, H.; Yam, V. W. W. *Dalton Trans.* **2007**, 3526.

(33) Casas, J. M.; Forniés, J.; Fuertes, S.; Martín, A.; Sicilia, V. *Organometallics* **2007**, *26*, 1674, and references therein.

(34) Díez, A.; Forniés, J.; Larraz, C.; Lalinde, E.; López, J. A.; Martín, A.; Moreno, M. T.; Sicilia, V. Submitted to *Inorg. Chem.*

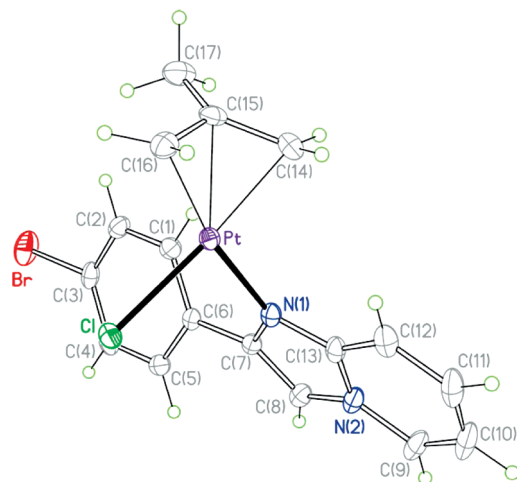
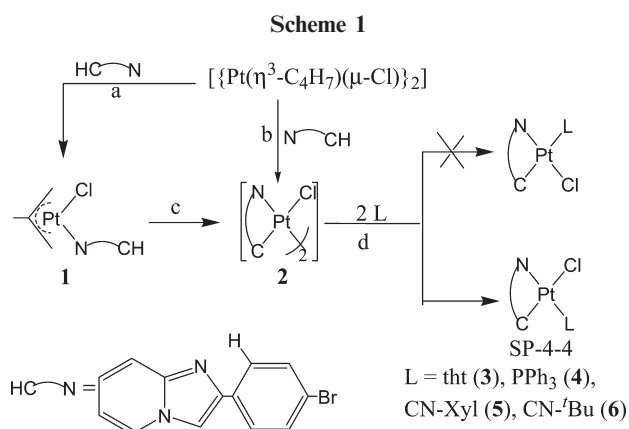


Figure 1. Molecular structure of complex **1**.



of a Pt–Cl terminal bond in *trans* position to a ligand with a large *trans* influence.³⁵ The presence of the allyl and the HC^N ligands was evident from the peak corresponding to [Pt(η³-C₄H₇)(HC^N)]⁺ observed in its MALDI (+) mass spectrum and corroborated by the X-ray study on a single crystal of it (Figure 1, Table 1). As can be seen, **1** is a mononuclear complex in which the platinum(II) center exhibits a highly distorted square-planar environment mainly due to the geometry and bonding mode of the η³-allyl group. The three Pt–C_{allyl} distances are roughly equal and shorter than those found in other η³-allyl platinum(II) and palladium(II) complexes containing ligands with a greater *trans* influence than Cl and N.^{36–38} The dihedral angle between the best plane defined for the 2-methylallyl moiety and the platinum coordination plane (Pt, Cl, N1, C14, C16) is 73.6(1)°. The Pt–Cl distance [2.368(7) Å] fits the Pt–Cl bond length [2.367(7) Å] found in the relevant complex [(η³-C₃H₅)Pt(P(^tBu)₃)Cl].^{39,40} The Pt–N bond length [2.092(25)

Table 1. Selected Structural Data for **1**

Bond Lengths [Å]			
Pt–C(14)	2.099(4)	Pt–C(16)	2.097(4)
Pt–C(15)	2.097(4)	Pt–Cl	2.368(7)
Pt–N(1)	2.092(3)	C(15)–C(16)	1.424(4)
C(14)–C(15)	1.427(5)	C(5)–C(17)	1.499(5)
C(6)–C(7)	1.472(4)	C(7)–C(8)	1.372(4)
N(1)–C(7)	1.382(4)	N(2)–C(8)	1.371(4)
N(1)–C(13)	1.338(4)	N(2)–C(13)	1.384(4)
N(2)–C(9)	1.380(4)		
Bond Angles [deg]			
N(1)–Pt–Cl	90.34(7)	N(1)–Pt–C(14)	99.94(11)
C(16)–Pt–Cl	99.65(9)	C(14)–C(15)–C(16)	114.1(3)
C(16)–C(15)–C(17)	122.2(3)	C(16)–Pt–C(14)	69.54(13)
		C(14)–C(15)–C(17)	122.3(3)

Å] is in the upper range of those observed in Pt(II) complexes with the same kind of ligands,^{41,42} in agreement with the high *trans* influence of the η³-2-methylallyl group.

The 2-(4-bromophenyl)imidazo[1,2-*a*]pyridine ligand is not planar; the phenyl ring forms an angle of 32.5(1)° with the best plane defined for the imidazo[1,2-*a*]pyridine fragment. Both parts of the ligand are almost perpendicular to the platinum coordination plane, the interplanar angles being 72.0(1)° and 69.6(1)° for the phenyl and imidazo[1,2-*a*]pyridine fragments, respectively. As can be seen, the phenyl ring is turned in such a way that the C1–H1 vector points toward the platinum atom. After locating the hydrogen atoms geometrically we found that the Pt···H1 distance was 2.78 Å and the Pt–H1–C1 angle was 120.9°. These parameters, together with the observed Pt···Cl separation [3.365(3) Å], are in the range observed for reported hydrogen bridging M···H–C bonds^{43,44} and differ from observed values for agostic systems.⁴⁵ Taking into account the presence, in the molecule, of two hydrogen bond acceptor atoms (Pt, Cl) and the nonhindered rotation of the phenyl ring around the C6–C7 bond, the existence of the Pt···H1 interaction could be considered as the step prior to the C1–H1 activation process, to give the cyclometalated complex, **2**.

In solution, all the NMR spectra display the expected signals for **1** in accordance with its X-ray structure. The H1 and H12 NMR signals (see Experimental Section and Scheme 2) appear downfield shifted (Δδ: 0.3 ppm H1, 0.67 ppm, H12) with respect to those in the free ligand, which is a characteristic feature of D–H···Pt hydrogen interaction involving the filled d_{z²} orbital of the Pt(II) center.^{43,46} As a consequence of the nonhindered rotation around the C6–C7 and Pt–N bonds, the protons H1 and H2 are chemically equivalent to H5 and H4 (appearing as an AA'XX' system) and so are C1 and C2 to C5 and C4. The methyl allyl group (η³-C₄H₇) gives five ¹H NMR signals, unambiguously

(35) Aucott, S. M.; Slawin, A. M. Z.; Woollins, J. D. *Eur. J. Inorg. Chem.* **2002**, 2408.

(36) Grassi, M.; Meille, S. V.; Musco, A.; Pontellini, R.; Sironi, A. J. *J. Chem. Soc., Dalton Trans.* **1989**, 615.

(37) Pandolfo, L.; Paiaro, G.; Dragani, L. K.; Maccato, C.; Bertani, R.; Facchin, G.; Zanotto, L.; Ganis, P.; Valle, G. *Organometallics* **1996**, *15*, 3250.

(38) Crociani, B.; Benetollo, F.; Bertani, R.; Bombieri, G.; Meneghetti, F.; Zanotto, L. *J. Organomet. Chem.* **2000**, *605*, 28.

(39) Carturan, G.; Belluco, U.; del Pra, A.; Zanotti, G. *Inorg. Chim. Acta* **1979**, *33*, 155.

(40) Mann, B. F.; Shaw, B. L.; Shaw, G. J. *J. Chem. Soc. A* **1971**, 3536.

(41) Pal, S.; Das, D.; Chattopadhyay, P.; Sinha, C.; Panneerselvam, K.; Lu, T.-H. *Polyhedron* **2000**, *19*, 1263.

(42) Chiu, B. K.-W.; Lam, M. H.-W.; Lee, D. Y.-K.; Wong, W.-Y. *J. Organomet. Chem.* **2004**, *689*, 2888.

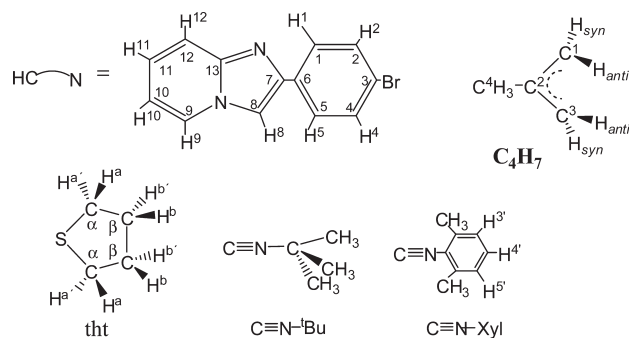
(43) Casas, J. M.; Forniés, J.; Martín, A. J. *J. Chem. Soc., Dalton Trans.* **1997**, 1559.

(44) Braga, D.; Grepioni, F.; Tedesco, E.; Biradha, K.; Desiraju, G. R. *Organometallics* **1997**, *16*, 1846.

(45) Crabtree, R. H.; Holt, E. M.; Lavin, M.; Morehouse, S. M. *Inorg. Chem.* **1985**, *24*, 1986.

(46) Brammer, L. *Dalton Trans.* **2003**, 3145.

Scheme 2. Numerical Scheme for NMR Purposes



assigned on the basis of a $^1\text{H}-^{13}\text{C}$ HSQC experiment, at 3.52 (1H *syn*), 3.0 (1H *syn*), 2.06 (1H *anti*), 1.98 (3H) and 1.65 ppm (1H *anti*), in agreement with the lack of symmetry in complex **1**. The high values of $J_{\text{Pt}-\text{H}}$ are similar to those found in other η^3 -allyl derivatives,^{39,40} including the starting complex $[\{\text{Pt}(\eta^3\text{-C}_4\text{H}_7)(\mu\text{-Cl})\}_2]$.⁴⁷ The presence of two resonances corresponding to C1' and C3' of the η^3 -C₄H₇ group with similar chemical shifts and Pt–C coupling constants agrees with the lack of symmetry in complex **1** and also with the symmetrically π -bonded 2-methylallyl ligand. The $J_{\text{Pt}-\text{C}}$ values are all smaller than those found in complex $[\{\text{Pt}(\eta^3\text{-C}_4\text{H}_7)(\mu\text{-Cl})_2\}]$,⁴⁸ as expected for the stronger *trans* influence of a N with respect to a Cl ligand.

As is usual in di- μ -chloro cyclometalated complexes, compound $[\{\text{Pt}(\text{C}^{\wedge}\text{N})(\mu\text{-Cl})\}_2]$ (**2**) is barely soluble in most common solvents, which precludes obtaining good ^{13}C or $^{195}\text{Pt}\{^1\text{H}\}$ NMR spectra. Its ^1H NMR was recorded in DMSO-*d*₆ as the solvent and provides direct evidence of the purity of the prepared sample, the elimination of the allyl group, and the metalation of the 2-(4-bromophenyl)imidazol[1,2-*a*]pyridine ligand (HC[^]N) through one *ortho*-C of the phenyl ring. Hence, in complex **2** H1 disappears and the remaining phenyl protons are all inequivalent to each other, giving three signals with their corresponding multiplicity proving the metalation of the HC[^]N group. In the solid state, the IR spectrum of **2** shows two $\nu(\text{Pt}-\text{Cl})$ absorptions at 320 and 261 cm^{-1} . These values are significantly higher than those described in the literature for the dinuclear complexes $[\{\text{Pt}(\text{P}^{\wedge}\text{C})(\mu\text{-Cl})\}_2]$ ($\text{P}^{\wedge}\text{C} = -\text{CH}_2\text{C}_6\text{H}_4\text{P}^i\text{Bu}(o\text{-tolyl})$, $-\text{CH}_2\text{C}_6\text{H}_4(\text{P}^i\text{Bu})_2$,⁴⁹ $-\text{CH}_2\text{C}_6\text{H}_4(o\text{-tolyl})_2$)⁵⁰, in agreement with the weaker *trans* influence of nitrogen compared to phosphorus. Thus, compound **2** is a five-membered cyclometalated compound resulting from the selective intramolecular activation of a C_{ph}–H bond of 2-(4-bromophenyl)imidazol[1,2-*a*]pyridine (HC[^]N) by the allyl complex $[\{\text{Pt}(\eta^3\text{-C}_4\text{H}_7)(\mu\text{-Cl})\}_2]$ followed by 2-methylpropene elimination. Other attempts to cyclometalate this HC[^]N ligand using K₂PtCl₄ and [PtCl₂(NCPPh)₂] as starting materials in refluxing 2-methoxyethanol failed; in all cases mixtures of **2** and other unidentified compounds precipitated in the reaction system and pure **2** could not be obtained. However the

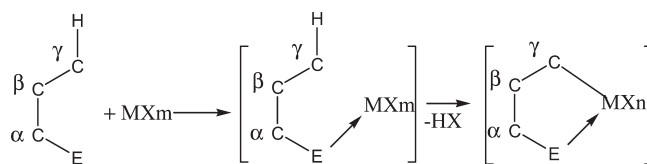
(47) ^1H NMR (CD₂Cl₂, 400.13 MHz, 298 K, δ): 3.58 (s, $^2J_{\text{Pt}-\text{H}} = 40$ Hz, 2H_{*syn*}), 2.11 (s, $^3J_{\text{Pt}-\text{H}} = 85.6$ Hz, 3H, Me), 2.04 (s, $^2J_{\text{Pt}-\text{H}} = 85.6$ Hz, 2H_{*anti*}).

(48) $^{13}\text{C}\{^1\text{H}\}$ NMR (CD₂Cl₂, 100.63 MHz, 298 K, δ): 110.33 (s, $J_{\text{Pt}-\text{C}} = 108$ Hz, C-2), 45.22 (s, $J_{\text{Pt}-\text{C}} = 281$ Hz, C-1, C-3), 22.62 (s, $J_{\text{Pt}-\text{C}} = 55$ Hz, C-4).

(49) Cheney, A. J.; Shaw, B. L. *J. Chem. Soc., Dalton Trans.* **1972**, 754.

(50) Forniés, J.; Martín, A.; Navarro, R.; Sicilia, V.; Villarroya, P. *Organometallics* **1996**, *15*, 1826.

Scheme 3



use of $[\{\text{Pt}(\eta^3\text{-C}_4\text{H}_7)(\mu\text{-Cl})\}_2]$ gave **2** as a pure solid in high yield, and no traces of oxidative addition products were observed. Hence, although the allyl complex $[\{\text{Pt}(\eta^3\text{-C}_4\text{H}_7)(\mu\text{-Cl})\}_2]$ is not as easy to prepare as other precursors for cyclometalation processes (e.g., K₂PtCl₄,^{51,52} [PtCl₂(NCPPh)₂],⁵⁰ [PtCl₂(dmsO)₂],^{53,54} [PtCl₂(SEt₂)₂]⁵⁵), it has proven to be a very convenient starting material⁵⁶ as in this case, given the selectivity and yield of the described reaction. Cyclometalation was generally considered to proceed by a two-step reaction mechanism (Scheme 3).¹ The intermediate coordination compounds have been detected^{57,58} and isolated⁵⁹ in the reactions of [Pt₂Me₂(μ -SMe₂)] with imines containing two nitrogen atoms, which coordinate to the metal center as chelate ligands. With imines containing only one single donor nitrogen such intermediates could never be isolated and could be detected only when the metalation step was hindered by bulky groups.^{59–61} Hence, cycloplatination intermediates containing the ligand coordinated through the N in a monodentate fashion have hardly ever been isolated.^{62–65} In some cases, no interaction between the later activated C \cdots H bond and the metal atom is observed,^{64,65} in others, such as the N-bound ferrocenylamine Pt(II) complexes, *trans*-[PtCl₂(DMSO)]($\eta^5\text{-C}_5\text{H}_4\text{-CH}_2\text{NMe}_2$)Fe($\eta^5\text{-C}_5\text{H}_5$)⁶² and $[\{\text{trans-PtCl}_2(\text{DMSO})\}_2\{\mu\text{-Fe}(\eta^5\text{-C}_5\text{H}_4\text{CH}_2\text{NMe}_2)\}_2]$,⁶³ a Pt \cdots H–C interaction can be adduced, although it is very weak since the Pt \cdots H distances are quite long, 3.1⁶³ or 3.38 Å.⁶² In our case, the use of $[\{\text{Pt}(\eta^3\text{-C}_4\text{H}_7)(\mu\text{-Cl})\}_2]$ as precursor has enabled us to isolate the cycloplatination intermediate $[\text{Pt}(\eta^3\text{-C}_4\text{H}_7)\text{Cl}(\text{HC}^{\wedge}\text{N-}\kappa\text{N})]$ (**1**), containing the HC[^]N- κ N ligand coordinated in a monodentate fashion and showing a clear Pt \cdots H–C interaction.

(51) Yeo, W.-C.; Vittal, J. J.; White, A. J. P.; Williams, D. J.; Leung, P.-H. *Organometallics* **2001**, *20*, 2167.

(52) Wu, L.-Y.; Hao, X.-Q.; Xu, Y.-X.; Jia, M.-Q.; Wang, Y.-N.; Gong, J.-F.; Song, M.-P. *Organometallics* **2009**, *28*, 3369.

(53) Meijer, M. D.; Kleij, A. W.; Williams, B. S.; Ellis, D.; Lutz, M.; L., S. A.; van Klink, G. P. M.; van Koten, G. *Organometallics* **2002**, *21*, 264.

(54) Crespo, M.; Anderson, C. M.; Tanski, J. M. *Can. J. Chem.* **2009**, *87*, 80.

(55) Wang, Z.; Sugiarti, S.; Morales, C. M.; Jensen, C. M.; Morales-Morales, D. *Inorg. Chim. Acta* **2006**, *359*, 1923.

(56) Pregosin, P. S.; Wombacher, F.; Albinati, A.; Lianza, F. *J. Organomet. Chem.* **1991**, *418*, 249.

(57) Anderson, C. M.; Crespo, M.; Font-Bardía, M.; Klein, A.; Solans, X. *J. Organomet. Chem.* **2000**, *601*, 22.

(58) Anderson, C. M.; Crespo, M.; Jennings, M. C.; Lough, A. J.; Ferguson, G.; Puddephatt, R. J. *Organometallics* **1991**, *10*, 2672.

(59) Crespo, M.; Font-Bardía, M.; Pérez, S.; Solans, X. *J. Organomet. Chem.* **2002**, *642*, 171.

(60) Crespo, M.; Solans, X.; Font-Bardía, M. *J. Organomet. Chem.* **1996**, *518*, 105.

(61) Crespo, M.; Martínez, M.; Sales, J.; Solans, X.; Font-Bardía, M. *Organometallics* **1992**, *11*, 1288.

(62) Ranatunge-Bandarage, P. R. R.; Robinson, B. H.; Simpson, J. *Organometallics* **1994**, *13*, 500.

(63) Ranatunge-Bandarage, P. R. R.; Duffy, N. W.; Johnston, S. M.; Robinson, B. H.; Simpson, J. *Organometallics* **1994**, *13*, 511.

(64) Wu, Y. J.; Ding, L.; Wang, H. X.; Liu, Y. H.; Yuan, H. Z.; Mao, X. A. *J. Organomet. Chem.* **1997**, *535*, 49.

(65) Ryabov, A. D.; Panyashkina, I. M.; Polyakov, V. A.; Fischer, A. *Organometallics* **2002**, *21*, 1633.

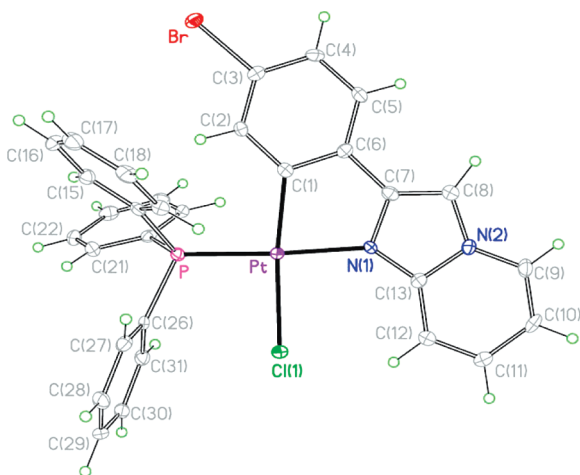


Figure 2. Molecular structure of complex **4**.

Reactivity of $[\{\text{Pt}(\text{C}^{\wedge}\text{N})(\mu\text{-Cl})\}_2]$ (2**) toward Monodentate S, P, and C Donor Ligands.** The dinuclear complex $[\{\text{Pt}(\text{C}^{\wedge}\text{N})(\mu\text{-Cl})\}_2]$ (**2**) reacts with several neutral monodentate S, P, and C donor ligands, such as tht, PPh_3 , CN-Xyl, and CN^tBu in a 1:2 molar ratio (Scheme 1d and Experimental Section) to give the mononuclear complexes $[\text{PtCl}(\text{C}^{\wedge}\text{N})\text{L}]$ (L = tht (**3**), PPh_3 (**4**), CN-Xyl (**5**), CN^tBu (**6**)), which were obtained as pure and air-stable solids in moderate to good yields and fully characterized by the usual means. All the spectroscopic data discussed below, relative to compounds **3–6**, indicate that the isomer SP-4-4 (*trans* C, Cl) is the only one present in each case, as is usual for this kind of compound.⁶⁶ Each compound, **3–6**, shows one $\nu_{\text{Pt-Cl}}$ absorption (278 cm^{-1} **3**, 283 cm^{-1} **4**, 285 cm^{-1} **5**, 284 cm^{-1} **6**) at similar frequencies to another, which are consistent with a terminal Pt–Cl bond *trans* to C.^{35,62,67} Complexes **5** and **6** additionally show one absorption assignable to $\nu_{\text{C}\equiv\text{NR}}$ (2179 cm^{-1} **5**, 2194 cm^{-1} **6**), at similar frequencies to those observed in other cyclometalated complexes with terminal $\text{C}\equiv\text{N-Xyl}$ and $\text{C}\equiv\text{N}^t\text{Bu}$ ^{29,68,69} and, as expected, at a higher frequency than in the corresponding free ligands ($\text{C}\equiv\text{N-Xyl}$: 2131 cm^{-1} , $\text{C}\equiv\text{N}^t\text{Bu}$: 2125 cm^{-1}).

Well-resolved ^1H NMR spectra of **3–6** show the signals due to the $\text{C}^{\wedge}\text{N}$ group and the corresponding co-ligand, L, unambiguously assigned on the basis of $^1\text{H}-^1\text{H}$ COSY experiments (see Experimental Section and Scheme 2). The most significant change with respect to the starting complex, **2**, is the significant upfield shift of the H2 signal in complex **4** (L = PPh_3), which has been ascribed to the anisotropic shielding effect of the aromatic ring current of a phenyl group in PPh_3 on the H2 pointing toward it.^{70–73} This is consistent

with the *cis* arrangement of the Pt–C and Pt–P bonds in the SP-4-4 isomer and can be seen in Figure 2. The observed values of $^3J_{\text{Pt-H}_2}$ are in all cases very similar to those found in the literature for related compounds.^{74,75} The $^{31}\text{P}\{\text{H}\}$ NMR spectrum of **4** shows a singlet with the expected platinum satellites; the Pt–P coupling constant value (4408 Hz) is in agreement with a *trans* arrangement of triphenylphosphine and the Pt–N bond.^{66,75,76} The $^{13}\text{C}\{\text{H}\}$ and $^{195}\text{Pt}\{\text{H}\}$ NMR spectra could be recorded for complexes **3** (L = tht) and **6** (L = CN^tBu) but not for **4** (L = PPh_3) and **5** (L = CN-Xyl) because of their low solubility in most common solvents. In each case their ^{195}Pt NMR spectra show a singlet; the $\delta(^{195}\text{Pt})$ for **6** (-3807 ppm) is upfield shifted with respect to that in **3** (-3646 ppm), as corresponds to the higher electron density of the metal center, in agreement with better σ -donor properties of the isocyanide ($\text{C}\equiv\text{N}^t\text{Bu}$) and its weak electron-withdrawing character. In both **3** and **6**, the $\delta(^{195}\text{Pt})$ values are similar to those observed in the literature for related platinum(II) complexes^{59,62,77} and are downfield shifted with respect to that of the unmetalated complex, **1**, which indicates a smaller electronic density on the platinum center in the metalated complexes.⁷⁸ This fact contrasts with the observed upfield shift of the ^{195}Pt signal upon metalation when another starting material, such as *trans*- $\text{PtCl}_2(\text{dmsO})_2$, is used in the process.⁶² The Pt–C coupling constant values for C13, C7, and C6 in complexes **3** (L = tht) and **6** (L = CN^tBu) are much higher than in complex **1**, containing the unmetalated $\text{HC}^{\wedge}\text{N-}\kappa\text{N}$ ligand; for the metalated carbon atom (C1) and the adjacent one (C2) the values are similar to those observed in other C,N-cyclometalated Pt(II) complexes.⁷⁹

The molecular structure of compound **4** was determined by X-ray diffraction studies (Figure 2, Table 2). As can be seen, the platinum(II) center exhibits a distorted square-planar environment due to the small bite angle of the cyclometalated ligand [$80.8(1)^\circ$]. This angle and the Pt– $\text{C}^{\wedge}\text{N}$ and Pt– $\text{N}^{\wedge}\text{C}$ bond lengths are similar to those observed in other five-membered metallacycles of Pt(II).^{28,29,53,73,80,81} A chloride and a triphenylphosphine ligand complete the coordination sphere of platinum(II). The Pt–Cl and Pt–P distances are in the range of Pt–Cl^{52,53,73,81,82} and Pt–P^{53,73,81–83} bonds *trans* to σ -carbon and nitrogen, respectively. As a consequence of the metalation, the two fragments of the metalated ligand, 4-bromophenyl and imidazol[1,2-*a*]pyridine, are coplanar to each other [the interplanar angle is $4.9(1)^\circ$] and also to the platinum coordination plane, the interplanar angles being $2.1(1)^\circ$ and $3.1(1)^\circ$, respectively. One of the phenyl rings

(74) Newman, C. P.; Casey-Green, K.; Clarkson, G. J.; Cave, G. W. V.; Errington, W.; Rourke, J. P. *Dalton Trans.* **2007**, 3170.

(75) Kleij, A. W.; Gebbink, R. J. M. K.; Lutz, M.; Li, S. A.; van Koten, G. J. *Organomet. Chem.* **2001**, 621, 190.

(76) Capapé, A.; Crespo, M.; Granell, J.; Font-Bardia, M.; Solans, X. *Dalton Trans.* **2007**, 2030.

(77) Mamtora, J.; Crosby, S. H.; Newman, C. P.; Clarkson, G. J.; Rourke, J. P. *Organometallics* **2008**, 27, 5559.

(78) Still, B. M.; Kumar, P. G. A.; Aldrich-Wright, J. R.; Price, W. S. *Chem. Soc. Rev.* **2007**, 36, 665.

(79) Cardenas, D. J.; Echevarren, A. M.; Ramirez de Arellano, M. C. *Organometallics* **1999**, 18, 3337.

(80) Forniés, J.; Fuertes, S.; Martín, A.; Sicilia, V.; Gil, B.; Lalinde, E. *Dalton Trans.* **2009**, 2224.

(81) Zucca, A.; Cinellu, M. A.; Minghetti, G.; Stoccoro, S.; Manassero, M. *Eur. J. Inorg. Chem.* **2004**, 4484.

(82) Martín, R.; Crespo, M.; Font-Bardia, M.; Calvet, T. *Organometallics* **2009**, 28, 587.

(83) Slater, J. W.; Lydon, D. P.; Alcock, N. W.; Rourke, J. P. *Organometallics* **2001**, 20, 4418.

(66) Otto, S.; Samuleev, P. V.; Polyakov, V. A.; Ryabov, A. D.; Elding, L. I. *Dalton Trans.* **2004**, 3662.

(67) Pregosin, P. S.; Wombacher, F. J. *Organomet. Chem.* **1991**, 418, 249.

(68) Lai, S. W.; Lam, H. W.; Lu, W.; Cheung, K. K.; Che, C. M. *Organometallics* **2002**, 21, 226.

(69) Lai, S. W.; Chan, M. C. W.; Cheung, K. K.; Che, C. M. *Organometallics* **1999**, 18, 3327.

(70) Smith, P. D.; Gelbrich, T.; Hursthouse, M. B. *J. Organomet. Chem.* **2002**, 659, 1.

(71) Craig, C. A.; Garces, F. O.; Watts, R. J.; Palmans, R.; Frank, A. J. *Coord. Chem. Rev.* **1990**, 97, 193.

(72) Mdleleni, M. M.; Bridgewater, J. S.; Watts, R. J.; Ford, P. C. *Inorg. Chem.* **1995**, 34, 2334.

(73) Zucca, A.; Petretto, G. L.; Stoccoro, S.; Cinellu, M. A.; Manassero, M.; Manassero, C.; Minghetti, G. *Organometallics* **2009**, 28, 2150.

Table 2. Selected Structural Data for **4**

Bond Lengths [Å]			
Pt–C(1)	2.030(3)	Pt–P	2.230(9)
Pt–N(1)	2.096(3)	Pt–Cl(1)	2.385(4)
C(6)–C(7)	1.452(5)	C(7)–C(8)	1.361(5)
N(1)–C(7)	1.382(4)	N(2)–C(8)	1.383(4)
N(1)–C(13)	1.352(4)	N(2)–C(13)	1.391(4)
N(2)–C(9)	1.367(4)		
Bond Angles [deg]			
C(1)–Pt–N(1)	C(1)–Pt–P(1)	N(1)–Pt–Cl(1)	
80.86(12)	95.66(10)	92.60(8)	
P–Pt–Cl(1)	C(13)–N(1)–Pt	C(7)–N(1)–Pt	
90.89(3)	139.6(2)	112.9(2)	
C(2)–C(1)–Pt	C(6)–C(1)–Pt		
130.0(2)	114.3(2)		

[C14–C19] in triphenylphosphine is oriented toward the C2–H2 bond, and the angle between this line and the perpendicular to that plane is 41.97°. Crystals of complex **6** were also obtained, but unfortunately the poor quality of the X-ray diffraction data obtained precludes complete structural determination. Nevertheless, atom connectivity can be established without error, showing a structure very similar to that of **4** with CN-¹Bu instead of PPh₃.

To summarize, all the spectroscopic and structural data discussed above indicate that in the cleavage of the bridging system in complex $[\{\text{Pt}(\text{C}^{\wedge}\text{N})(\mu\text{-Cl})\}_2]$ (**2**) by the neutral ligands tht, PPh₃, CN-Xyl, and CN-¹Bu only one (SP-4-4) of the two possible isomers (Scheme 1) is formed selectively. This result is compatible with the expected degree of transphobia (T)^{33,84,85} of pairs of *trans* ligands, $T[\text{C}(\text{C}^{\wedge}\text{N})/\text{L}(\text{Cl})] < T[\text{C}(\text{C}^{\wedge}\text{N})/\text{L}(\text{S}, \text{P}, \text{C})]$, taking into account that the greater the *trans* influence^{86,87} of two ligands, the greater the transphobia. Given that in complexes **3–6** there is no steric hindrance between pairs of *cis* ligands, the resulting geometry (*trans* C, Cl) is that expected from the electronic preferences.

Preliminary studies on compounds **1–6** indicate that only the mononuclear complexes $[\text{PtCl}(\text{C}^{\wedge}\text{N})\text{L}]$ (L = CN-Xyl (**5**), CN-¹Bu (**6**)) are luminescent. Both contain a σ Pt–C_{CAN} bond and a strong-field ligand, L, such as isocyanide. Hence absorption and emission spectra studies were carried out only on them, in both the solid state and solution.

Absorption Spectra and Theoretical Calculations. Considering the low solubility of **5** in common organic solvents and for comparative purposes, we obtained the absorption spectra of **5**, **6**, and the unmetalated ligand HC[^]N in different solvents at low concentration (5×10^{-5} M) (Table S1, Figure S1 for **5** and Figure 3 for **6**).

In the HC[^]N ligand, as in compounds **5** and **6**, all the absorptions appeared at $\lambda < 360$ nm with $\epsilon \geq 1 \times 10^4$ M⁻¹

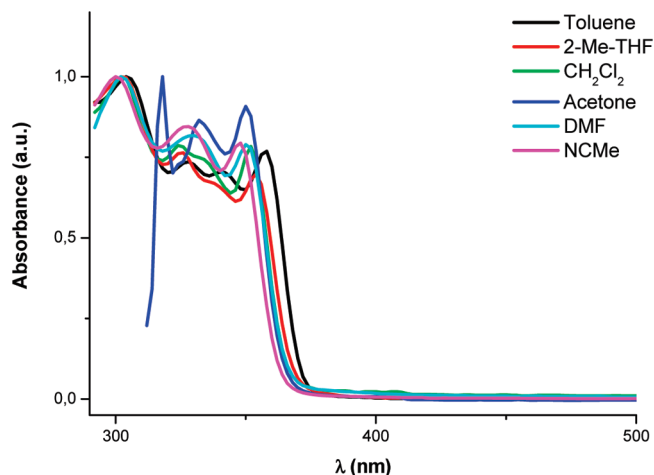


Figure 3. Normalized UV-vis spectra of complex **6** (5×10^{-5} M) in different solvents.

cm^{-1} , which we have tentatively assigned to metal-perturbed ligand-centered transitions (¹LC π – π^*) within the C[^]N ligand.^{27,29,68,88–90} In contrast to most C[^]N-cyclometalated Pt(II) complexes, in these cases no absorptions in the 370–450 nm range with extinctions between 2000 and 6000 M⁻¹ cm⁻¹ assigned as metal-to-ligand charge transfer (MLCT) transitions^{29,90–92} were observed. To shed some light on this, theoretical calculations using the time-dependent density functional theory (TD-DFT) were carried out for **6** at the SAOP/TZP level of theory. The optimized S₀ structure and geometrical parameters (Figure S2a and Table S2) agree well with the experimental values. All the relevant data about the molecular orbitals (MOs) involved in the excited states and the calculated electronic excitations appear in Figure S3 and Tables S3–S6. In toluene solution the HOMO (Figure 4 and Table S4) is mostly constructed from orbitals located on the phenyl ring of the C[^]N (78%) with small contribution of the chloride ligand (4%) and the Pt center (3%), while the LUMO is well located on the pyridinic and imidazolyl rings of the C[^]N ligand (87%), with a very low contribution of both Pt and CN¹Bu. The contribution of Pt and Cl orbitals increases on going from the HOMO to HOMO–1 and HOMO–2. Similar relative compositions of the frontier orbitals have been found in imine-^{29,34,88} or pyrazol-based⁹³ cyclometalated platinum(II) complexes. Figure 4 shows the calculated excited states in toluene solution (bars) that fit well, within the accuracy of the method, with the experimental absorptions in the region of $\lambda > 290$ nm. Calculations indicate that the major contribution to the lowest-lying absorption ($\lambda = 356$ nm) involves the HOMO → LUMO (81%) and HOMO–1 → LUMO (9.4%) transitions, indicating a remarkable intraligand (¹IL, C[^]N) character mixed with small MLCT/L[^]LCT, since this band also involves transitions $d_{\text{Pt}} \rightarrow \pi^*_{\text{C}^{\wedge}\text{N}}$ and $\pi^*_{\text{Cl}} \rightarrow \pi^*_{\text{C}^{\wedge}\text{N}}$. Calculations also show a lower IL and larger MLCT/L[^]LCT character of the absorption bands located at higher energies (350 nm > λ > 290 nm). The same assignments could be made for the absorptions observed for complex **5**, since they

(84) Vicente, J.; Arcas, J. A.; Martínez-Viviente, E.; Jones, P. G. *Organometallics* **2002**, *21*, 4454.

(85) Vicente, J.; Arcas, J. A.; Gálvez-López, M. D.; Jones, P. G. *Organometallics* **2006**, *25*, 4247.

(86) Pregosin, P. S. *Transition Metal Nuclear Magnetic Resonance*; Elsevier: New York, 1991.

(87) Cotton, F. A. *Chemistry of Precious Metals*; Blackie Academic & Professional, Chapman & Hall: London, 1997.

(88) Shao, P.; Li, Y.; Azenkeng, A.; Hoffmann, M. R.; Sun, W. *Inorg. Chem.* **2009**, *48*, 2407.

(89) Qiu, D.; Wu, J.; Xie, Z.; Cheng, Y.; Wang, L. *J. Organomet. Chem.* **2009**, *694*, 737.

(90) Schneider, J.; Du, P.; Jarosz, P.; Lazarides, T.; Wang, X.; Brennessel, W. W.; Eisenberg, R. *Inorg. Chem.* **2009**, *48*, 4306.

(91) Brooks, J.; Babayan, Y.; Lamansky, S.; Djurovich, P. I.; Tsyba, I.; Bau, R.; Thompson, M. E. *Inorg. Chem.* **2002**, *41*, 3055.

(92) Schneider, J.; Du, P.; Wang, X.; Brennessel, W. W.; Eisenberg, R. *Inorg. Chem.* **2009**, *48*, 1498.

(93) Develay, S.; Blackburn, O.; Thompson, A. L.; Williams, J. A. G. *Inorg. Chem.* **2008**, *47*, 11129.

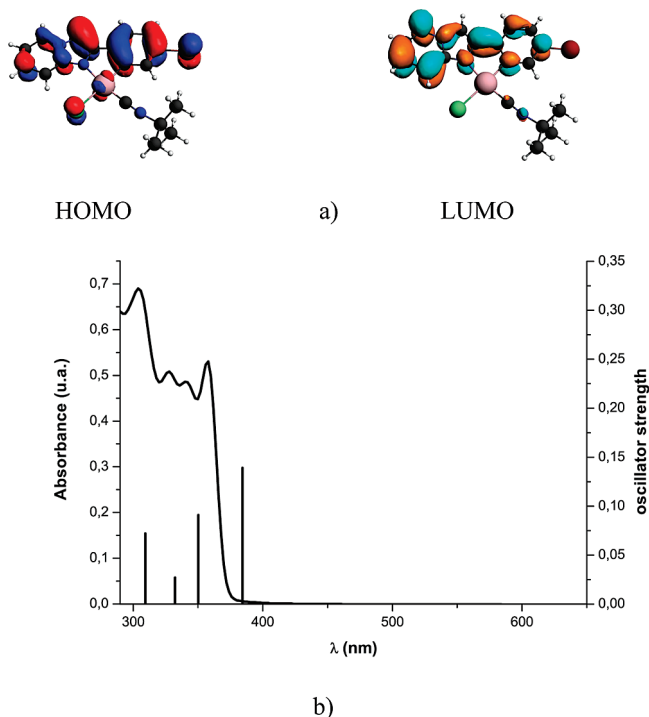


Figure 4. (a) Frontier orbitals plots for complex **6** in toluene obtained by DFT. (b) Calculated absorption spectrum (bars) and experimental UV-vis spectrum of **6** in toluene (5×10^{-5} M).

appear at similar wavenumbers in toluene. The charge transfer (CT) nature of these bands is consistent with their blue-shift in the simulated absorption spectrum of **6** in a more polar solvent, such as acetonitrile, and causes the modest negative solvatochromism^{29,88} observed experimentally for **5** and **6** (Table S1, Figure S1 for **5** and Figure 3 for **6**). For both complexes **5** and **6** the lowest-lying absorption band follows Beer's law in a wide concentration range (352 nm, DMF, 4×10^{-5} to 2×10^{-3} M, **5**; 352 nm, CH_2Cl_2 , 2×10^{-5} to 1×10^{-2} M, **6**), suggesting that no remarkable aggregation occurs within this range (see Figures S4 and S5).^{29,34} The UV-vis spectra of compounds **5** and **6** both in solution and in the solid state (Figure S6) barely show any influence at all of the isocyanide substituent (xylil or *tert*-butyl) in the lower-energy bands, in agreement with the noncontribution of MOs located on these co-ligands on the HOMOs of these complexes.

Emission Spectroscopy and Theoretical Calculations. Solution and Glass State. Complexes $[\text{PtCl}(\text{C}^{\wedge}\text{N})(\text{CN-Xyl})]$ (**5**) and $[\text{Pt}(\text{C}^{\wedge}\text{N})(\text{Cl})(\text{CN-}^t\text{Bu})]$ (**6**) are slightly emissive in solution at both room (298 K) and low (77 K) temperature. The results are summarized in Table 3. In dilute solution (5×10^{-5} M) both complexes show (Figure 5 for **5** and Figures 6 and S7 for **6**) only one high-energy (HE) emission band ($\lambda_{\text{max}} = 367$ nm, $\lambda_{\text{exc}} = 300$ nm **5**; $\lambda_{\text{max}} = 376$ nm, $\lambda_{\text{exc}} = 340$ nm **6**) that can be reasonably attributed to IL emissive states from the $\text{C}^{\wedge}\text{N}$ ligand considering the emission spectrum of the unmetalated ligand ($\text{HC}^{\wedge}\text{N}$) in fluid CH_2Cl_2 solution (Figure S8). In a more concentrated solution (10^{-3} M) the emission of **5** changes with the excitation wavelength. The excitation band corresponding to the unstructured low-energy (LE) emission appears greatly red-shifted with respect to that for the HE emission of the monomers. This fact, together with the color of the emission and its appearance at high concentration, suggests that it is presumably due to emissive ground-state aggregates generated by weak $\text{Pt} \cdots \text{Pt}$ and/or $\pi-\pi$ interactions of aromatic groups,

as frequently occurs in square-planar Pt(II) complexes, although the existence of excimer-like emissions cannot be excluded.^{20,28,29,93-96} Thus, this emission is tentatively assigned to ${}^3\text{MMLCT}/{}^3\pi-\pi^*$ transitions.

The emission intensity of the HE band for complexes **5** and **6** decreases at high concentrations,⁸⁸ as illustrated in Figure S9 for complex **6**. Investigation of the dependence of the emission lifetime (τ_{obs}) on the concentration for **5** and **6** measured at 376 nm (Figures S10, S11) shows values of τ_0 and self-quenching constant (K_Q) in line with those reported for related Pt(II) complexes.^{34,93,96}

Both complexes **5** and **6** become more emissive upon cooling. The emission spectra of **6** at low temperature (77 K) show the same profile in diluted (5×10^{-5} M) or concentrated (10^{-3} M) solution in CH_2Cl_2 (Figure S6). They exhibit a broad phosphorescent band at low energy (LE) ($\lambda_{\text{max}} = 580$ nm) in addition to a low-intensity band at 450 nm, which can be selectively obtained upon excitation at 300 nm a concentrated solution of **6** (10^{-3} M) in 2-Me-thf at 77 K (Figure 7). The peak maxima (456, 486, and 522 nm), vibronic progressions (ca. 1400 cm^{-1} , typical of breathing modes on aromatic rings), and long lifetime point to an emission arising mainly from a ${}^3\text{IL}$ excited state with a slight, if any, ${}^3\text{MLCT}$ character,^{91,94,97} as in the analogous complexes $[\text{Pt}(\text{bzq})\text{Cl}(\text{CNR})]$ ($\text{R} = {}^t\text{Bu}, \text{Xyl}$).³⁴ The excitation spectra in 2-Me-thf monitoring the LE band ($\lambda_{\text{max}} = 580$ nm) at 10^{-3} M resemble the lower-energy absorption observed in the UV-visible spectrum of **6**. Aiming to know the origin of these emission bands theoretical calculations were carried out on complex **6**. The optimized structural parameters of **6** in the S_0 and T_1 states computed at the BP86/TZP level are given in Figure S2. Structural changes occurring upon the $\text{S}_0 \rightarrow \text{T}_1$ excitation are small (0.1–0.25 Å for the bond lengths and $0.2-1.3^\circ$ for the bond angles).

Natural bond orbital (NBO) analysis has been employed to estimate the changes of the natural atomic charges upon the $\text{S}_0 \rightarrow \text{T}_1$ excitation of **6**; the values are shown in Figure S12a. In general, it was found that charge is primarily transferred from the chloride ligand and the platinum central atom toward the $\text{C}^{\wedge}\text{N}$ ligand and, to a lesser extent, toward the $-\text{C}\equiv\text{N}-$ group of the $\text{CN-}^t\text{Bu}$ ligand.

The simulated emission spectra of **6** by using time-dependent density functional theory (TD-DFT) calculations at the SAOP/TZP level are depicted schematically in Figure S13. The calculated emission maximum, λ_{max} , at 575 nm is in excellent agreement with the phosphorescence emission maximum observed experimentally at 77 K (580 nm CH_2Cl_2 , 587 nm 2-Me-thf). This band could be attributed to a $\text{SOMO}-1 \leftarrow \text{SOMO}$ electronic transition. The calculated band maximum around 475 nm, found to be in close agreement with those observed experimentally at $\lambda = 450$ or 456 nm in a rigid matrix of CH_2Cl_2 or 2-Me-thf, respectively, originates primarily from a $\text{SOMO}-1 \leftarrow \text{LUMO}+1$ electronic transition. Moreover, the emission bands with maxima around 330 and 260 nm mainly arise from $\text{SOMO}-2 \leftarrow \text{LUMO}$ and $\text{SOMO}-2 \leftarrow \text{LUMO}+5$ transitions,

(94) Ma, B.; Li, J.; Djurovich, P. I.; Yousufuddin, M.; Bau, R.; Thompson, M. E. *J. Am. Chem. Soc.* **2005**, *127*, 28.

(95) Du, P.; Schneider, J.; Brennessel, W. W.; Eisenberg, R. *Inorg. Chem.* **2008**, *47*, 69.

(96) Williams, J. A. G.; Beeby, A.; S., D. E.; Weinstein, J. A.; Wilson, C. *Inorg. Chem.* **2003**, *42*, 8609.

(97) Chang, C.-F.; Cheng, Y.-M.; Chi, Y.; Chiu, Y. C.; Lin, C. C.; Lee, G. H.; Chou, P. T.; Chen, C. C.; Chang, C. H.; Wu, C. C. *Angew. Chem., Int. Ed.* **2008**, *47*, 4542.

Table 3. Emission Data for Complexes 5 and 6

compound	color	media	λ_{em} [nm]	τ [μ s]		
5	light gray	solid (298)	575, 620 _{max} , 676 (λ_{ex} 400)	0.18 (620)		
		solid (77)	481, 522 _{max} , 564 (λ_{ex} 350)	341 (40%), 63.8 (60%) (522)		
		CH ₂ Cl ₂ 5 × 10 ⁻⁵ M (298)	337 _{sh} , 367 _{max} (λ_{ex} 300)	0.1 (367)		
		CH ₂ Cl ₂ 5 × 10 ⁻⁵ M (77)	467, 557, 640 (λ_{ex} 400), 633 (λ_{ex} 480)	24.8 (95%), 138.7 (5%) (467); 1.4 (557); 4.2 (633)		
		CH ₂ Cl ₂ 10 ⁻³ M (298)	380 _{max} , 399, 456 _{sh} (λ_{ex} 330); 639 (λ_{ex} 420)	92 ns (380); 0.9 (639)		
		CH ₂ Cl ₂ 10 ⁻³ M (77)	603 _{max} (λ_{ex} 450)	2.7 (97%), 20.9 (3%) (603)		
		6	pale yellow	solid (77)	484, 521 _{max} , 563 (λ_{ex} 350); 495 _{sh} , 529 _{sh} , 561 _{max} (λ_{ex} 400)	198.7 (26%), 30.7 (74%) (521); 225 (18%), 15.2 (82%) (561)
				CH ₂ Cl ₂ 5 × 10 ⁻⁵ M (298)	360 _{sh} , 376 _{max} , 392, 418 _{sh} (λ_{ex} 340)	0.1 (376)
				CH ₂ Cl ₂ 5 × 10 ⁻⁵ M (77)	450, 457 _{sh} , 580 _{max} (λ_{ex} 350)	92.1 (46%), 348 (54%) (450); 181 (18%), 24.9 (82%) (580)
				CH ₂ Cl ₂ 10 ⁻³ M (298)	376 (λ_{ex} 320)	0.1 (376)
CH ₂ Cl ₂ 10 ⁻³ M (77)	450, 459 _{sh} , 580 _{max} (λ_{ex} 350)			304 (59%), 38.2 (41%) (450); 32.3 (84%), 275 (16%) (580)		
2-metilthf 5 × 10 ⁻⁵ M (298)	335 _{sh} , 358 _{sh} , 375 _{max} , 393 _{sh} (λ_{ex} 300)			0.1 (375)		
2-metilthf 5 × 10 ⁻⁵ M (77)	543 _{sh} , 578 _{max} , 612 _{sh} (λ_{ex} 330)			289 (75%), 37.8 (25%) (578)		
2-metilthf 10 ⁻³ M (298)	380 _{max} , 394 (λ_{ex} 330)			0.1 (380)		
2-metilthf 10 ⁻³ M (77)	456, 486 _{max} , 522 (λ_{ex} 300); 552 _{sh} , 587 _{max} , 617 (λ_{ex} 360)			403.2 (456); 161.5 (23%), 414.5 (77%) (486); 270 (35%), 35.7 (65%) (587)		

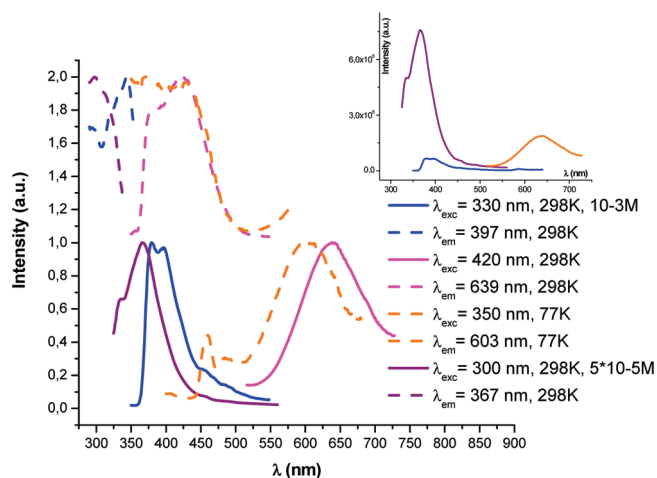


Figure 5. Normalized excitation and emission spectra of **5** in CH₂Cl₂ at 298 and 77 K. Inset: Unnormalized emissions in the same conditions.

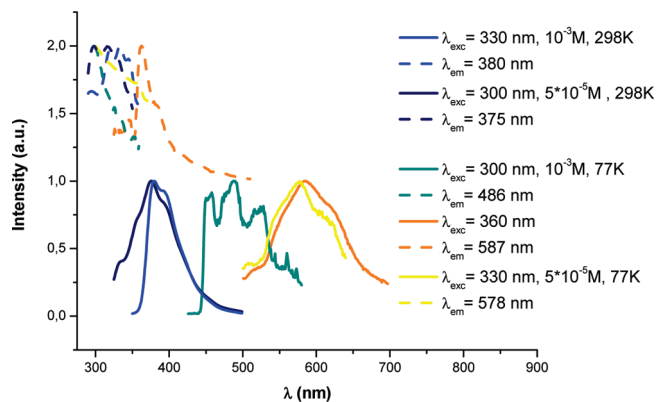


Figure 6. Normalized excitation and emission spectra of **6** in 2-Me-thf.

respectively. In view of the MOs participating in the electronic transitions (Figure S12) it can be concluded that the T₁ to S₀ de-excitation in the gas phase corresponds to a ligand (C[^]N) to metal (Pt) to ligand (Cl) charge transfer transition. Hence, the

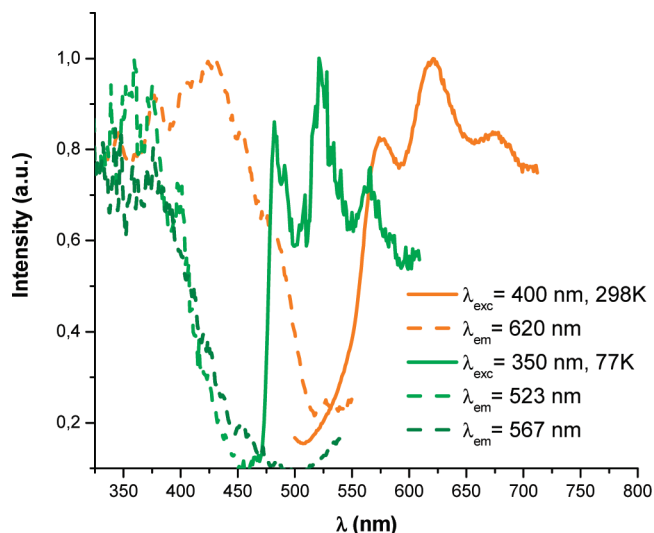


Figure 7. Normalized excitation and emission spectra of **5** in the solid state.

emission at 580 nm seems to be due to a ³L/MLCT excited state. However, taking into account that with the inclusion of solvent molecules in the calculations, the Cl orbital contribution to the HOMO diminishes with respect to the gas phase (the HOMO is mostly constructed from orbitals located on the phenyl ring of the C[^]N with marginal contribution of the chloride ligand and the Pt center), it seems reasonable to consider this low-energy emission as a mixed ³IL/³L/MLCT transition.

Solid State. In the solid state, complex **5** exhibits “luminescent thermochromism” (Figure 8) presumably related to the existence or absence of Pt···Pt and/or π–π interactions.⁸⁰ Thus at 298 K complex **5** exhibits an intense orange-red luminescence band centered at 620 nm, which changes to a green phosphorescence band upon cooling. The differences in their excitation spectra indicate that both emissions are due to two different excited states.⁸⁰ The excitation profile of the HE band (observable at 77 K) resembles the UV–vis spectrum of **5**. This fact, the vibronic spacing (1540, 1230 cm⁻¹), and lifetime are typical of ³IL localized on the C[^]N ligand with low, if any, contributions of

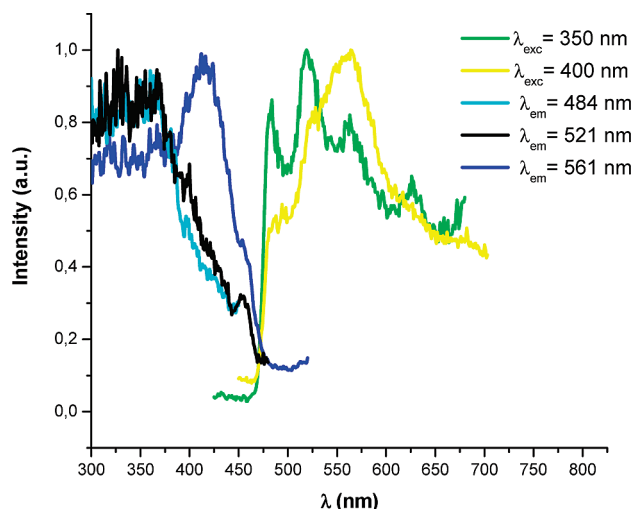


Figure 8. Normalized excitation and emission spectra of **6** in the solid state at 77 K.

³MLCT transitions in the monomer species.^{34,91,94,97} This assignment is well supported in view of the emission spectrum of the unmetalated (HC[^]N) ligand in the solid state at 77 K (Figure S14). However, the energy of the orange-red emission, the lifetime, and the excitation profile monitoring at 620 nm are similar to those of the LE emission observed in fluid CH₂Cl₂ at 10⁻³ M, which has been tentatively assigned to excited states of aggregates generated by Pt···Pt and/or π-π interactions (³MMLCT/³π-π*).^{20,28,29,93-95} However, in the solid state, complex **6** is only luminescent at 77 K (Figure 8). It is probable that the high energy of the excited state brings it sufficiently close to higher-lying metal-centered states, which provide it with a thermally activated nonradiative decay pathway.⁹³ As can be seen, the emission profile changes with the excitation wavenumber. The vibronic band observed upon exciting at 350 nm seems to be due to two phosphorescent emissions, a green high-energy (HE) band with λ_{max} = 521 nm and a minor contribution of a low-energy (LE) band centered at 561 nm that becomes the more important one upon exciting at 400 nm. Both emissions resemble those of **6** in glassy 2-Me-thf (10⁻³ M). The green emission has been assigned mainly to ³IL excited states and the LE one to mixed ³IL/³L'MLCT transitions, all corresponding to monomer species. The excitation profile of the LE band shows a peak maxima ca. 3000 cm⁻¹ red-shifted with respect to the excitation maxima of this band in glassy 2-Me-thf. Therefore the contribution of ³MMLCT/³π-π* excited states to the low-energy part of this band cannot be excluded.

Conclusions

Complex [{Pt(η³-C₄H₇)(μ-Cl)}₂] has been proved to be a very convenient starting material for cyclometalation of 2-(4-bromophenyl)imidazol[1,2-*a*]pyridine (HC[^]N) in view of the selectivity and yield of the process to give [{Pt(C[^]N)(μ-Cl)}₂] (**2**). Compound **2** was obtained from [{Pt(η³-C₄H₇)(μ-Cl)}₂] and HC[^]N in a one-pot reaction in refluxing 2-methoxyethanol or step-by-step through the intermediate [Pt(η³-C₄H₇)Cl(HC[^]N-κN)] (**1**). Complex **1** precipitates in the reaction mixture if [{Pt(η³-C₄H₇)(μ-Cl)}₂] and HC[^]N are reacted in refluxing acetone. The X-ray structural data in complex **1** indicate the existence of a weak Pt···H-C

hydrogen bridging bond (*d*Pt···H1 = 2.78 Å, *d*Pt-C1 = 3.365(3) Å, angle Pt-H1-C1 = 120.9°) in agreement with the observed ¹H NMR data. Taking into account the presence in the molecule of two hydrogen bond acceptor atoms (Pt, Cl) and the nonhindered rotation of the phenyl ring around the C6-C7 bond, the existence of the Pt···H1 interaction could presumably be considered as the prior step for the C1-H1 activation process. The cleavage of the bridging system in [{Pt(C[^]N)(μ-Cl)}₂] (**2**) by the neutral ligands L rendered the mononuclear complexes [PtCl(C[^]N)L] (L = tht (**3**), PPh₃ (**4**), CN-Xyl (**5**), CN-^tBu (**6**)) with the geometry (*trans* C, Cl) expected from the electronic preferences, taking into account the degree of transphobia (*T*) of pairs of *trans* ligands, $\tau[\text{C}(\text{C}^{\wedge}\text{N})/\text{L}(\text{Cl})] < \tau[\text{C}(\text{C}^{\wedge}\text{N})/\text{L}(\text{S}, \text{P}, \text{C})]$.

Only complexes [PtCl(C[^]N)(CNR)] (R = Xyl (**5**), ^tBu (**6**)) are luminescent, both of which contain two strong-field ligands, a σ Pt-C_{C[^]N} bond and a strong-field isocyanide ligand. The change of the isocyanide substituent (xylyl or *tert*-butyl) hardly causes any effect on the absorption bands of compounds **5** and **6** both in solution and in the solid state, in agreement with the noncontribution of MOs located on these co-ligands on the HOMOs of these complexes. Complex **6** shows phosphorescence at 77 K both in solution and in the solid state with the emissions arising from ³IL and ³L'MLCT excited states of monomer species. Complex **5** exhibits “luminescent thermochromism” in the solid state; at 77 K it shows a green phosphorescence band assigned to ³IL transitions located on the C[^]N group of monomer species, while at 298 K an orange-red emission is observed, being tentatively assigned to excited states of emissive aggregates (³MMLCT/³π-π*) generated by Pt···Pt and/or π-π interactions in view of the emission and excitation energy maxima. Thus, the “luminescent thermochromism” shown by **5** in the solid state seems to be related to the existence or absence of these kinds of interactions among monomer species.

With the aim of obtaining luminescent compounds containing 2-(4-bromophenyl)imidazol[1,2-*a*]pyridine-*k*C,N, the synthesis and characterization of new heteroleptic complexes containing different ancillary ligands are in progress.

Experimental Section

All the information about materials, instrumentation methods used for characterization and photophysical studies, computational details concerning TD-DFT calculations, and the X-ray structure analysis of **1** and **4**·CHCl₃ together with the full IR and NMR data corresponding to HC[^]N and complexes **1-6** is given in the Supporting Information.

Synthesis of [Pt(η³-C₄H₇)Cl(HC[^]N-κN)] (1**).** An orange solution of [{Pt(η³-C₄H₇)(μ-Cl)}₂] (0.286 g, 0.5 mmol) in acetone (20 mL) containing 2-(4-bromophenyl)imidazol[1,2-*a*]pyridine (0.273 g, 1 mmol) was refluxed for 1 h. Within this process time, **1** precipitated as a white solid, which was filtered and washed with Et₂O. Yield: 0.27 g, 95%. Anal. Calcd for **1**, C₁₇H₁₆BrClN₂Pt (558.76): C, 36.54; H, 2.89; N, 5.01. Found: C, 36.37; H, 2.93; N, 4.96. MS (MALDI+): *m/z* 523 [Pt(HC[^]N)(η³-C₄H₇)]⁺.

Synthesis of [Pt(C[^]N)(μ-Cl)}₂] (2**): Method A.** An orange solution of [{Pt(η³-C₄H₇)(μ-Cl)}₂] (0.571 g, 1 mmol) in 2-methoxyethanol (20 mL) containing 2-(4-bromophenyl)imidazol[1,2-*a*]pyridine (HC[^]N, 0.546 g, 2 mmol) was refluxed for 2 h. The dark brown solid that precipitated was filtered and washed with MeOH and Et₂O, **2**. Yield: 0.74 g, 74%. **Method B.** A white suspension of [Pt(η³-C₄H₇)Cl(HC[^]N-κN)] (**1**) (0.447 g, 0.80 mmol) in 2-methoxyethanol (20 mL) was refluxed for 2 h, and the resulting solid was filtered and washed with Et₂O (20 mL) to give a dark brown solid, **2**. Yield: 0.32 g, 82%. Anal. Calcd for **2**,

$C_{26}H_{16}Br_2Cl_2N_4Pt_2$ (1005.32): C, 31.06; H, 1.60; N, 5.57. Found: C, 30.95; H, 1.77; N, 5.78.

Synthesis of [PtCl(C[^]N)(tht)] (3). tht (53.58 μ L, 0.6067 mmol) was added to a stirred suspension of **2** (0.30 g, 0.3038 mmol) in CH_2Cl_2 (15 mL). The reaction mixture was refluxed for 5 h, cooled to room temperature, and filtered through Celite. The resulting solution was evaporated to dryness and the residue washed with Et_2O (2×5 mL), yielding **3** as a gray solid. Yield: 0.15 g, 42%. Anal. Calcd for $BrC_{17}ClH_{16}N_2PtS$: C, 34.61; H, 2.73; N, 4.75; S, 5.43. Found: C, 35.04; H, 2.59; N, 4.72; S, 5.42. MS (MALDI+): m/z 555 [Pt(C[^]N)(tht)]⁺.

Synthesis of [PtCl(C[^]N)(PPh₃)] (4). PPh₃ (111.58 mg, 0.4254 mmol) was added to a stirred suspension of **2** (210.00 mg, 0.2127 mmol) in CH_2Cl_2 (30 mL), and the reaction mixture was refluxed for 3 h and then cooled to room temperature. The resulting precipitate was filtered off and washed with CH_2Cl_2 (2×5 mL) and Et_2O (2×5 mL) to afford **4** as a gray solid. Yield: 0.30 g, 92%. Anal. Calcd for $BrC_{31}ClH_{23}N_2P_3$: C, 48.68; H, 3.03; N, 3.66. Found: C, 48.27; H, 2.86; N, 3.44. MS (MALDI+): m/z 728 [Pt(C[^]N)(PPh₃)]⁺, 502 [Pt(C[^]N)]⁺.

Synthesis of [PtCl(C[^]N)(CN-Xyl)] (5). CN-Xyl (0.1020 g, 0.7775 mmol) was added to a stirred suspension of **2** (0.3838 g, 0.3887 mmol) in CH_2Cl_2 (20 mL) at room temperature. After 18 h the precipitate was filtered off and washed with CH_2Cl_2 (2×5 mL) and Et_2O (2×5 mL) to afford **5** as a light gray solid. Yield: 0.29 g, 60%. Anal. Calcd for $BrC_{22}ClH_{17}N_3Pt$: C, 41.69; H, 2.70; N, 4.42. Found: C, 41.47; H, 2.63; N, 4.67. MS (MALDI+): m/z 598 [Pt(C[^]N)(CN-Xyl)]⁺.

Synthesis of [PtCl(C[^]N)(CN-^tBu)] (6). CN-^tBu (77.13 μ L, 0.6828 mmol) was added to a stirred suspension of **2** (0.34 g, 0.3414 mmol) in $CHCl_3$ (30 mL). The reaction mixture was refluxed for 10.5 h, cooled to room temperature, and filtered through Celite. The resulting solution was evaporated to dryness and the residue washed with Et_2O (3×5 mL), yielding **6** as a pale yellow solid. Yield: 0.29 g, 73%. Anal. Calcd for $BrC_{18}ClH_{17}N_3Pt$: C, 36.91; H, 2.93; N, 7.17. Found: C, 36.78; H, 3.41; N, 7.02. MS (MALDI+): m/z 550 [Pt(C[^]N)(CN-^tBu)]⁺, 494 [Pt(C[^]N)(CN)]⁺.

Acknowledgment. This work was supported by the Spanish MICINN (Project CTQ2008-06669-C02-01) and the Gobierno de Aragón (Grupo de Excelencia: Química Inorgánica y de los Compuestos Organometálicos).

Supporting Information Available: Absorption data (Table S1). Normalized UV-vis spectra of complex **5** in different solvents and HC[^]N and **6** in toluene (Figure S1). Selected structural parameters of the ground state, S_0 , and first triplet excited state, T_1 , calculated at the BP86/TZP level (Figure S2) of complex **6**. Cartesian coordinates of the stationary points on the PES of complex **6** in the S_0 ground state (Table S2). 3D contour plots of all MOs involved in the electronic transitions in the simulated absorption spectra of complex **6** (Figure S3). Molecular orbital energies, compositions, and assignment calculated for the ground state, S_0 , of **6** at the SAOP/TZP level (Tables S3, S4, and S5). Principal singlet-singlet optical transitions ($f > 0.03$) calculated for the absorptions of complex **6** (Table S6). Normalized UV-vis absorption spectra at several concentrations at 298 K of **6** in CH_2Cl_2 (Figure S4) and **5** in DMF (Figure S5). Diffuse reflectance UV-vis spectra in the solid state of **5**, **6**, and HC[^]N at 298 K (Figure S6). Emission spectra of **6** (Figure S7) and HC[^]N (Figure S8). Emission spectra of complex **6** in deoxygenated CH_2Cl_2 solutions at room temperature in different concentrations (Figure S9). Plot of the measurement luminescence decay constants versus concentration for **6** (Figure S10) and **5** (Figure S11). Natural atomic charges for the S_0 and T_1 states of **6**, spin density isosurface (0.002 au), and 3D contour plots of the relevant MOs calculated at the BP86/TZP level (Figure S12). Calculated emission spectra of **6** (Figure S13). Emission spectra of HC[^]N in the solid state (Figure S14). General procedures and materials, computational details, X-ray structure analysis of **1** and **4**· $CHCl_3$ (including Table S7), full IR and NMR data for HC[^]N and for **1**–**6**. Crystallographic data in CIF format. This material is available free of charge via the Internet at <http://pubs.acs.org>.